

Spatial Heterogeneity in Tumor Perfusion Measured with Functional Computed Tomography at 0.05 μ l Resolution¹

Leena M. Hamberg,² Paul E. G. Kristjansen,² George J. Hunter, Gerald L. Wolf, and Rakesh K. Jain

Center for Imaging and Pharmaceutical Research, Department of Radiology, Massachusetts General Hospital and Harvard Medical School, Boston, Massachusetts 02129-2060 [L. M. H., G. J. H., G. L. W.], and Steele Laboratory, Department of Radiation Oncology, Massachusetts General Hospital and Harvard Medical School, Boston, Massachusetts 02114 [P. E. G. K., R. K. J.]

Abstract

High speed (200 ms temporal resolution) functional computed tomography was used to demonstrate tumor vascular heterogeneity with 0.05 μ l spatial resolution. Vascular topologies were investigated in 2 human small cell lung cancer lines implanted either s.c. or as a tissue isolated preparation in immunocompromised mice. Peripheral versus central vascular topology was identified in the s.c. and tissue-isolated preparations, respectively. Pharmacokinetic analysis demonstrated that tumor physiology was influenced by cell line ($P = 0.016$) and not by location ($P > 0.6$). This new technique has the potential to characterize individual tumors in patients with minimal invasiveness, permitting more detailed prognosis and management.

Introduction

Tumor blood flow and vascular morphology play an important role in tumor growth, metastasis, detection, and treatment. In particular, knowledge of the vascular state of a tumor may facilitate development of novel strategies for cancer therapy. In any individual case, it may also be possible to offer a more accurate prognosis by taking into account vascular pathophysiology of tumors *in situ* (1-4). Currently, quantitative information on the vascular physiology of tumors in a clinical setting is obtained either by counting the vascular density of biopsied tissue (4) or by noninvasive imaging of perfusion using magnetic resonance imaging, positron emission tomography or conventional CT³ (2, 5, 6). The former is invasive and limited to regions of the tumor which are biopsied. The latter techniques suffer from poor spatial and temporal resolution. Recently developed CT scanners utilizing slip-ring technology permit very high spatial resolution (<0.05 μ l) images to be obtained at rapid intervals (<100 ms), because the X-ray tube can rotate continuously around an object, making possible uninterrupted data acquisition. The combination of the high spatial and temporal resolutions makes this tool (fCT) an ideal method for the investigation of tissue vascular physiology, allowing the measurement of contrast agent pharmacokinetics and biodistribution *in vivo* (7). In the present study we have used clinically available contrast agents as vascular markers to investigate and measure the topography and regional distribution of perfusion in solid tumors. Ideally, based on vascular physiology, tumors can be divided in two categories: peripheral and central (8). Subcutaneous tumors are normally peripherally perfused while tissue-isolated tumors are usually centrally perfused (9, 10). Therefore, the model used to verify the value of this novel technology was small cell lung cancer implanted in immunodeficient nude mice, either s.c. in the flank or as a tissue-isolated tumor

(10). Two different human small cell lung cancer lines (CPH 54A and 54B), originally derived from the same tumor (11) were used. These two tumor lines have different physiological and pharmacokinetic characteristics (12, 13). Our goal was to find out whether or not this technology can discover these differences.

Materials and Methods

Tumor Lines. The human small cell lung cancer lines CPH 54A and 54B are propagated *in vitro* as continuous cell cultures and *in vivo* in immunodeficient mice. The original tumor was histologically classified as an intermediate type small cell lung cancer (11). The histological appearance has not changed during serial transplantation and propagation in nude mice.

In Vivo Preparation. Tumors were implanted in 8-10-week-old female NCr/Sed-nu/nu athymic mice, bred in the Edwin L. Steele Laboratory's animal facility (Massachusetts General Hospital, Boston, MA). Body weight ranged between 20 and 25 g. All animals were fed sterilized standard laboratory rodent chow and sterilized water *ad libitum*. Prior to all surgical or invasive procedures, the animals were anesthetized with a s.c. injection of ketamine (10 mg/kg) and xylazine (1 mg/kg) in 0.9% NaCl solution. Institutional guidelines for animal welfare and experimental conduct were followed. Tumors were prepared both as conventional s.c. flank implants and as tissue-isolated xenografts, following a recently developed procedure (10) that is based on an original preparation in rats (14, 15). After 21-28 days of tumor growth, the animals had a PE-10 catheter surgically inserted into their left carotid artery. Catheter patency was maintained by a heparinized 0.9% NaCl solution. Following this procedure the mean arterial blood pressures stayed at ≥ 80 mm Hg. This catheter was used for injection of iodinated contrast material into the circulation.

Computed Tomography. Imaging was performed using a CT system (TCT900S/xII; Toshiba, Tokyo, Japan). Each study consisted of a multislice axial image set to define anatomy and a single slice dynamic acquisition to monitor the passage of contrast material through tissues. The latter took advantage of the pharmacokinetics of iodinated contrast material specifically to image regional vascular physiology within the tumor.

Functional Imaging Protocol. After catheterization the anesthetized animal was positioned in the center of the CT scanner on a heating pad maintained at 37 °C. An anterior-posterior scout image was taken and used to choose 2-mm axial slices through the tumors. The imaging parameters for all the studies were 120 keV tube voltage, 150 mA tube current, and high resolution imaging mode, resulting in over 4 million data samples being acquired within a 360-degree tube rotation lasting 1 s. All images were reconstructed onto a 512- \times -512-image matrix using an 80-mm field of view. This gave a 0.16- \times -0.16-mm pixel size. The 2-mm slice voxel therefore represented 0.049 μ l of tissue. From the precontrast axial slices, a suitable slice containing the maximum amount of abnormal tissue in the field was selected for the functional study.

The functional study was performed in two parts: an initial acquisition to characterize early vascular behavior; and a delayed acquisition to characterize contrast agent washout from the tumor. For the initial acquisition, imaging was started 5 s before a 200- μ l bolus of iodinated contrast agent (Hypaque 76%; Winthrop-Brean Laboratories, New York, NY) manually injected into the carotid artery. The serial passage of contrast agent through the aorta and tumor vasculature was recorded. The aortic phase is very rapid compared to contrast agent washin and washout in the tumor; this required the first 20 s of image

Received 10/3/94; accepted 10/20/94.

The costs of publication of this article were defrayed in part by the payment of page charges. This article must therefore be hereby marked *advertisement* in accordance with 18 U.S.C. Section 1734 solely to indicate this fact.

¹ Supported by R35-CA-56591 to R. K. J.

² L. M. H. and P. E. G. K. contributed equally to this work.

³ The abbreviations used are: CT, slip-ring computed tomography; fCT, functional computed tomography; ROI, region of interest.

data to be collected continuously. After this rapid initial phase (but still part of the same acquisition) image data were collected once every 5 s (9 animals) or 15 s (4 animals). This gave a total imaging time of either 260 or 660 s for the first dynamic acquisition.

When data acquisition stopped and image reconstruction was complete (approximately 5 min), a new set of images with improved temporal resolution (200 ms between images) was reconstructed from the raw data obtained in the first 20 s of the study (7). A final temporal resolution of 200 ms was used in order to fully characterize the shape of the arterial input curve. The second dynamic acquisition was started as rapidly as technical factors permitted (typically 20 min after the injection of contrast material). At this time, 60 images were acquired with a 10-s delay between sequential images; no further contrast was injected.

Data Analysis. For image postprocessing, data were transferred from the CT scanner to a MacIntosh IICI computer (Apple, Inc., Cupertino, CA). Image sets were rearranged into their correct temporal order and extracted into a minimal matrix size that preserved all the data of interest.

A ROI was defined in the aorta to characterize the shape of the arterial input curve. For each tumor, data from five regions of interest were obtained. Four of these were concentric rings with inner and outer radii at 0–25, 25–50, 50–75, and 75–100% of the radius of the tumor. The fifth ROI was placed over the area of greatest contrast intensity and corresponded to the most vascular parts of the tumor. From these regions of interest, signal intensity-time curves were constructed and converted into concentration-time curves with the aid of a linear calibration curve obtained in a conventional manner from external standards (16).

These tumor concentration-time curves were then fitted, using a nonlinear algorithm, to the mathematical expression of a two-compartment model defined by

$$Y(t) = A \cdot (1 - e^{-k_1 t}) \cdot e^{-k_2 t} \quad (\text{A})$$

where A , k_1 , and k_2 are fitting parameters (17, 18). The constant A represents the maximal concentration of contrast agent in the tumor in the absence of washout and is dependent on the amount of contrast agent given. The next term defines contrast agent uptake into the tumor and the final term describes the clearance of contrast agent from the tumor; k_1 and k_2 are the respective rate constants for these two processes. To eliminate the effects of slightly varying doses, the tumor concentration-time curves were normalized using the area under the arterial input function, measured from the aorta, corrected for recirculation using the γ variate function.

$$C_A(t) = K^*(t - \tau)^\alpha * e^{-(t-\tau)/\beta} \quad (\text{B})$$

K is a constant scale factor, α and β are arbitrary parameters, and τ is the arrival time of the contrast agent into the tissue (19). After fitting, the area under the curve representing the amount of contrast agent injected, was calculated using the fitting parameters and the analytical formula

$$\text{Area} = K * \beta^{\alpha+1} * e^{\Gamma(\alpha+1)} \quad (\text{C})$$

where Γ is the Gamma function. The normalization for dose delivered was incorporated into the constant A which becomes A_{norm} .

The vascular topology in each tumor was determined by visually inspecting the images. The vascular physiology in different anatomical locations of the tumor was quantitatively compared using the parameters, A_{norm} , k_1 , and k_2 . These parameters reflect the vascular permeability vascular surface area and blood flow in the tumor. The parameters were used to compare s.c. with isolated and type 54A with type 54B tumors. Vascular distribution profiles were generated using the derived parameter $A_{\text{norm}} * k_1$, presented as an average, from the concentric ROIs for the s.c. and isolated tumors. $A_{\text{norm}} * k_1$ is the initial uptake slope of contrast agent into the tumor.

Results

Twenty-one tumors in 13 animals were studied. In eight animals both isolated and s.c. tumors were present. Four animals had only an isolated tumor and one animal had only a s.c. tumor. Of the 12 isolated tumors 7 were cell type 54B and 5 were cell type 54A small cell lung cancer. Four of nine s.c. tumors were type 54B and five were type 54A. In 3 s.c. tumors only 1 peripheral and central ROI pair was drawn because the mass was too small for further subdivision.

Visual inspection of the data revealed heterogeneity of tumor vascularity both within a tumor and between different tumors. Unequivocal differences in the appearance of the vascular topology could be identified between the isolated and s.c. tumors. The isolated tumors showed predominantly central vascularization, while s.c. tumors were rather more peripherally vascularized. Hypoperfused areas were found peripherally in the isolated tumors and centrally in the subcutaneous tumors. Fig. 1 provides an examples of these vascular differences in the two locations. Heterogeneity was demonstrated not only between different tumors but also within a tumor. Fig. 2 is an example of the heterogeneity of vascular physiology present within an isolated tumor. Three hemodynamically different regions are shown with the corresponding contrast response curves after conversion to concentration-time values. Highly perfused areas can be easily separated from hypoperfused, necrotic, or partially necrotic areas with this technique. Seventy-two % of the ROIs were well perfused in isolated tumors and 50% in s.c. tumors.

The average vascular distribution profiles for s.c. and isolated tumors are shown in Fig. 3. The patterns reflect the differences in distribution of blood supply, with a more central supply present in the isolated tumor, while the s.c. tumors derive their blood supply from the periphery, making central areas less well perfused.

Analysis of variance was performed on the hemodynamic parameters (i.e., A_{norm} , k_1 , and k_2) obtained from areas of greatest contrast intensity. The effects of location, s.c. versus isolated, and tumor type, 54A versus 54B, were compared. A quantitative comparison of the perfusion parameters is presented in Fig. 4. No significant differences were recorded between s.c. and isolated tumors as a whole ($P > 0.6$). A significant difference ($P < 0.02$) between cell lines was observed for the parameter A_{norm} . Nonsignificant differences between the cell types were observed for k_1 and k_2 ($P = 0.06$ in both cases). These data imply that a significantly higher peak concentration of contrast agent was achieved in the type 54A tumors.

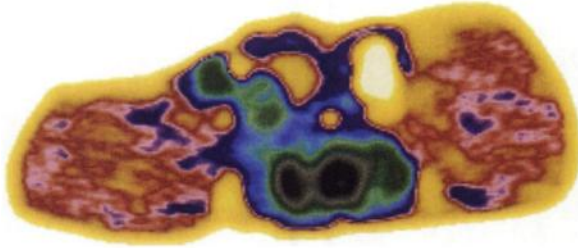
Discussion

The importance of tumor heterogeneity as a factor influencing the response to treatment is well described (2–4). We report an important advance in the application of new computed tomography technology which overcomes the limitations of spatial and temporal fidelity inherent in scintigraphy and magnetic resonance imaging; we call this functional or parametric CT (fCT). Early studies measuring physiological parameters with CT were limited to scan rates of 2–10 images/min and spatial resolution of 2–3 mm within a 5-mm slice. With the application of slip-ring technology and improvements in detector design, continuous, high spatial resolution data acquisition became possible, and we have been able to obtain image data with a temporal resolution approaching 1 ms and a spatial resolution of 0.16 mm within a 1-mm slice. Fortunately it is unnecessary to generate images very ms in order to demonstrate a dynamic process. Nyquist's sampling theorem states that "the entire information content of a dynamic process can be recorded by sampling it at a rate equal to, or greater than twice the maximum frequency contained within that process" (20). The implications of this theorem are that as long as changes in the dynamic process of interest are recorded at least twice as fast as

Tumor Location

Subcutaneous

Isolated




Low  High
Contrast Uptake

Fig. 1. Pseudocolored axial CT-image of an animal into which both s.c. and isolated tumors have been implanted. The isolated tumor was prepared by mobilizing the ovarian fat pad, seeding tumor into it, and then wrapping the preparation in paraffin film. This scheme results in a single artery and vein supplying and draining the tumor. The color scale represents the degree of contrast uptake into tissue, and as such reflects delivery of blood. Note that in the isolated tumor there is a peripheral rim of dark red and yellow, with areas of blue and magenta in the center. In the s.c. tumor the reverse is true with a central area of yellow and dark red and peripheral areas of dark blue and magenta. In this way it may be clearly appreciated that in the s.c. tumor the periphery is more vascularized than the hypoperfused center. In the isolated tumor hypoperfused areas are located mainly in the periphery in contrast to highly perfused areas in the center.

Tumor Perfusion Distribution

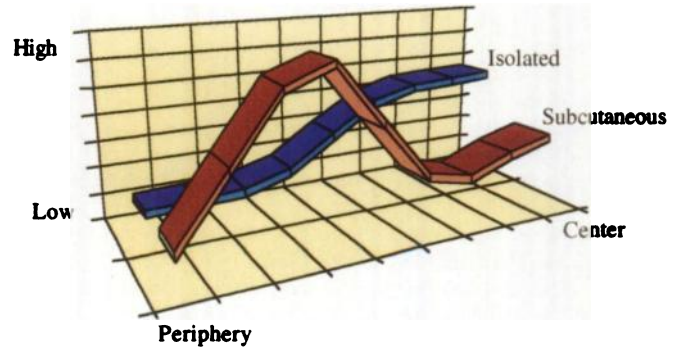


Fig. 3. For each tumor a washin index ($A_{norm} \cdot k_1$) was calculated as a function of the index at the center. Average values of this index were obtained for the s.c. and tissue-isolated tumors as a function of distance from the center of the tumor. The radial distribution of tissue perfusion is shown in the two tumor groups. Note the difference in distribution of perfusion indices in the two tumor locations. The s.c. tumors had proportionally increased peripheral perfusion as compared with the area of increased perfusion located centrally in the tissue-isolated tumors. These patterns of perfusion distribution reflect the differences in origin of blood supply in the two locations: the tissue-isolated tumors obtain their supply from a central stalk, while the s.c. tumors have a predominantly capsular blood supply.

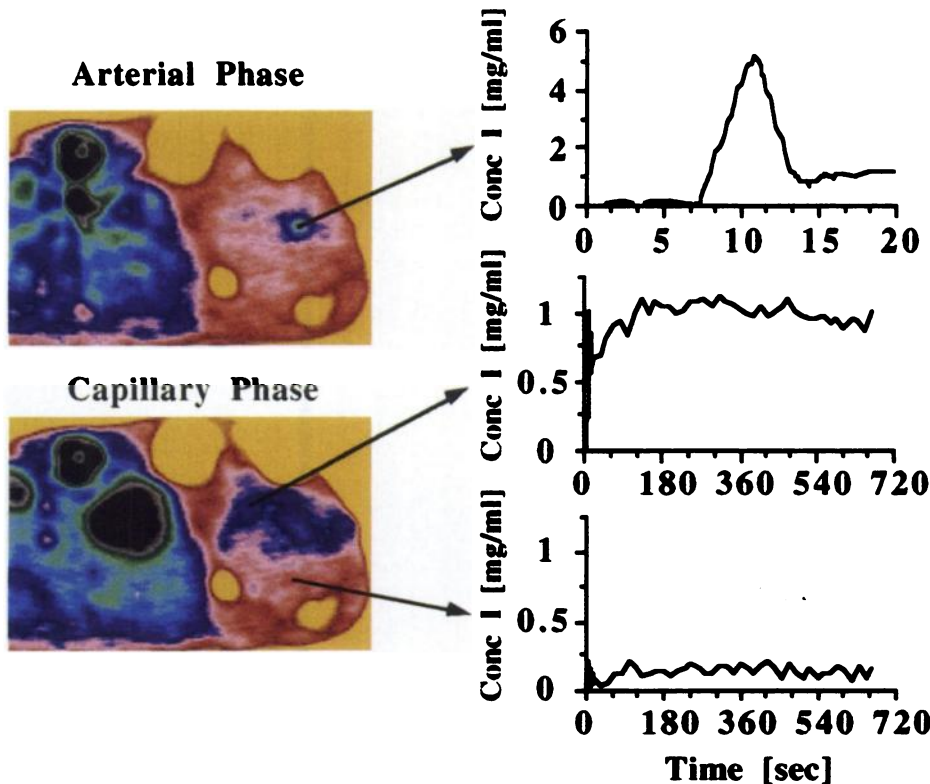


Fig. 2. The two images represent early and late frames from a continuous dynamic fCT acquisition. An isolated tumor has been used to demonstrate the three types of tissue response observed during the study. The top graph (red) is taken from the pedicle containing the feeding vessel; it shows a typical arterial input curve with a 5- to 6-s duration. The middle graph (blue) is the curve obtained from an area of tumor activity. It is typical of the uptake and washout recorded from actively perfused tumor. The bottom graph (green) demonstrates the vascular characteristics of an area of poor perfusion or necrosis. Arrows. The areas from which the curves were obtained. Note the different time scales for the arterial and capillary graphs.

they occur, then no information will be missed during the recording. Elsewhere we have shown that for dynamic events such as passage of contrast through a large artery, an acquisition rate of 5 images/s is within the Nyquist limit and is sufficient to capture all the information of interest,⁴ thus in the current study, when we resampled the initial 20 s

of 360-degree raw data we did so at 200-ms intervals without loss of information. This combination of spatial (0.049 μ l) and temporal (200 ms) resolution is among the highest achieved with any presently available, noninterventional imaging technique.

Of further interest is the measurement of chemotherapeutic agent pharmacokinetics directly within a tumor. The contrast material we used in this study, Hypaque 76, has a molecular weight of 614, is

⁴ G. J. Hunter, unpublished data.

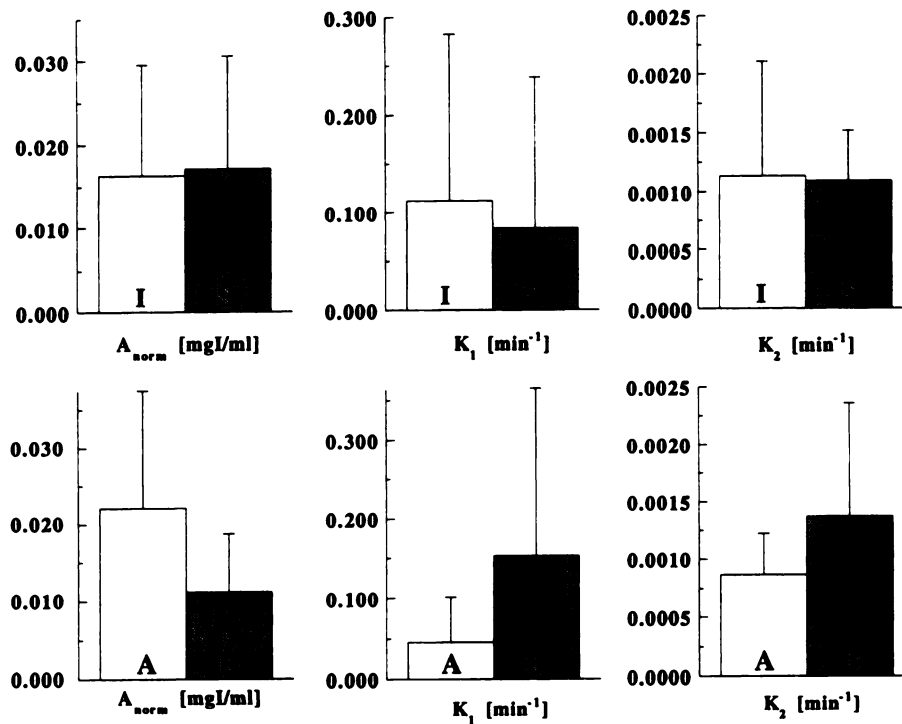


Fig. 4. For each parameter (A_{norm} , k_1 , and k_2) obtained from the fitting of a two compartment model to the hemodynamics of the active portion of each tumor, two null hypotheses were evaluated: (a) there is no difference in hemodynamic response observed between s.c. and tissue-isolated tumors irrespective of cell line; and (b) there is no difference in hemodynamic response observed between the cell lines 54A and 54B, irrespective of location. Analysis of variance, taking into account differences in observed variances, rejected the null hypothesis in case 2 (P values for A_{norm} , k_1 , and k_2 were 0.01, 0.06, and 0.06, respectively) and did not reject the null hypothesis in case 1 (P values for A_{norm} , k_1 , and k_2 were 0.9, 0.6, and 0.9, respectively). This implies that location is not an important factor in determining tumor vascular behavior, while differences in perfusion characteristics were observed between the 54A and 54B cell lines of human small cell lung cancer.

minimally protein bound, and is 99% excreted by passive filtration via the glomerulus. As a small particle in tissue, its mass behavior may be monitored using functional CT, and its tumor pharmacokinetics may be classified using a tracer kinetic approach with a two compartment model. In particular the combination of fCT and conventional contrast agents allows detailed study of regional tumor response to delivery of contrast material as well as defining the temporal characteristics of tumor heterogeneity. We believe that such analysis may predict the behavior of chemotherapeutic agents with similar chemical and physiological profiles to CT contrast agents (21). Naturally the effects of plasma protein binding need to be considered; however, such effects are easily incorporated into the kinetic analysis and do not detract from the ability to predict regional chemotherapeutic effects within a tumor.

The pharmacokinetics of contrast material and chemotherapeutic agents are not uniquely defined by making measurements at one or a few time points. It is clear that as contrast material enters the blood stream and interacts with tissue there are several phases in the measurement of change in drug concentration in the blood and tissue. Initially, high concentrations fall rapidly due to distribution within the vascular space. In order to capture these rapid changes, our imaging protocol acquired continuous data at an effective rate of 5 images/s for a total of 20 s. The second phase of drug pharmacokinetics is due to distribution into and interaction with tissues. The third phase is governed by drug elimination from the body. The latter two phases occur more slowly than the vascular distribution and do not require such rapid imaging. In our studies we reduced the imaging rate to 4 images/min but continued imaging for 10 min to capture the details of tissue interaction with the drug. In essence we captured the first pass characteristics of contrast agent pharmacokinetics, including measurement of a true arterial concentration-time curve, as well as being able

to delineate the slower, but more prolonged phases of contrast-tissue interaction.

In order to evaluate fCT as a method for investigating tumor vascular physiology and drug pharmacokinetics, we used two tumor implantation sites and two tumor cell lines. Previous work using invasive methods has suggested spatial heterogeneity of tumor structure; the concept of a necrotic core is well accepted (9). fCT has enabled us to interrogate the vascular structure of the tumors with much higher spatial resolution. The use of both s.c. and tissue isolated tumors allowed us to investigate the impact of tumor site on vascular physiology, and we were able to confirm that fCT can demonstrate the predicted differences in blood supply occasioned by the predominantly central, pedicle-based supply of the tissue-isolated tumor when compared with the predominantly peripheral blood supply of the s.c. implanted tumor. We were also able to identify regional differences in distribution of vascular supply in both the tissue isolated and s.c. tumors. On the basis of temporal separation we were able to identify the unique pedicular blood supply of the tissue-isolated models. Using simple compartmental analysis we were able to show regional differences in contrast agent pharmacokinetics. Analysis of the calculated parameters confirmed that the 54A and 54B tumor lines could be distinguished on the basis of their response to contrast agent. Interestingly it was shown that the site of implantation did not alter the expression of the tumor in terms of its pharmacokinetic interaction with the contrast agent. Interpretation of the pharmacokinetic data must be made with some understanding of the interaction among the parameters k_1 , k_2 , and A_{norm} . Examination of the k_1 and k_2 in isolation does not reveal a difference between the two cell lines ($P = 0.06$). However, both k_1 and k_2 influence the value of A_{norm} , and this parameter is significantly different in the two cell lines ($P = 0.016$). These differences in A_{norm} result from, and are consistent with, the

known multifactorial nature of the drug pharmacokinetics in these two cell lines (13).

In summary we have shown that fCT with contrast agent injection is capable of investigating regional tumor characteristics, allowing measurement of spatial and temporal events with 0.049 μ l and 200-ms resolution, respectively. The fine structure of implanted tumors was demonstrated as well as the differences in pharmacokinetic response in two cell lines. The ability of fCT to provide this information with very high resolution is complementary to the clinical availability of this method and the contrast agents used. By using functional computed tomography it may become possible to define optimal treatment strategies for unique tumor/patient combinations.

Acknowledgments

We thank Dr. Elkan Halpern for expert statistical guidance and Sylvie Roberge for her help in the tumor preparation.

References

- Jain, R. K. Determinants of tumor blood flow: a review. *Cancer Res.*, 48: 2641–2658, 1988.
- Vaupel, P., and Jain, R. K. *Tumor Blood Flow and Metabolic Microenvironment: Characterization and Implications for Therapy*. New York: Fischer Publishers, 1991.
- Jain, R. K. Physiological resistance to the treatment of solid tumors. *In: B. A. Teicher (ed.), Drug Resistance in Oncology*, pp 87–105. New York: Marcel Dekker, Inc., 1993.
- Folkman, J. Tumor angiogenesis. *In: J. F. Holland (ed.), Cancer Medicine*, Ed. 3, pp. 153–170. Philadelphia: Lea and Febiger, 1993.
- Eskey, C. J., Koretsky, A. P., Domach, M. M., and Jain, R. K. 2H-nuclear magnetic resonance imaging of tumor blood flow: spatial and temporal heterogeneity in a tissue-isolated mammary adenocarcinoma. *Cancer Res.*, 52: 6010–6019, 1992.
- Lammertsma, A. A. Positron emission tomography and *in vivo* measurements of tumour perfusion and oxygen utilisation. *Cancer Metastasis Rev.*, 6: 521–539, 1987.
- Hamberg, L. M., Hoop, B., Hunter, G. J., and Wolf, G. L. Functional imaging with slip-ring CT and echo planar MRI: a preliminary report. *Med. Rev.*, 49: 10–19, 1994.
- Rubin, P., and Cassaret, G. Microcirculation of tumors. I. Anatomy, function, and necrosis. *Clin. Radiol.*, 17: 220–229, 1966.
- Less, J. R., Skalak, T. C., Sevick, E. M., and Jain, R. K. Microvascular architecture in a mammary carcinoma: branching patterns and vessel dimensions. *Cancer Res.*, 51: 265–273, 1991.
- Kristjansen, P. E. G., Roberge, S., Lee, I., and Jain, R. K. Tissue-isolated human tumor xenografts in athymic nude mice. *Microvasc. Res.*, in press, 1994.
- Engelholm, S. A., Videløv, L. L., Spang-Tomsen, M., Brønner, N., Tommerup, N., Nielsen, M. H., and Hansen, H. H. Genetic instability of cell lines derived from a single human small cell carcinoma of the lung. *Eur. J. Cancer Clin. Oncol.*, 21: 815–824, 1985.
- Kristjansen, P. E. G., Spang-Thomsen, M., and Quistorff, B. Different energy metabolism in two human small cell lung cancer subpopulations examined by ³¹P magnetic resonance spectroscopy and biochemical analysis *in vivo* and *in vitro*. *Cancer Res.*, 51: 5160–5164, 1991.
- Kristjansen, P. E. G., Quistorff, B., Spang-Thomsen, M., and Hansen, H. H. Intratumoral pharmacokinetic analysis by ¹⁹F-magnetic resonance spectroscopy and cytostatic *in vivo* activity of gemcitabine (dFdC) in two small cell lung cancer xenografts. *Ann. Oncol.*, 4: 157–160, 1993.
- Gullino, P. M. Techniques to study of tumor pathophysiology. *In: H. Busch (ed.), Methods in Cancer Research*, pp. 45–91. New York: Academic Press, 1970.
- Gullino, P. M., and Grantham, F. H. Studies on the exchange of fluids between host and tumor. I. A method for growing “tissue-isolated” tumors in laboratory animals. *J. Natl. Cancer Inst.*, 27: 679–693, 1961.
- Gado, M. H., Phelps, M. E., and Coleman, R. E. An extravascular component of contrast enhancement in cranial computed tomography. *Radiology*, 117: 589–593, 1975.
- Lassen, N. A., and Perl, W. *Tracer Kinetics Methods in Medical Physiology*. New York: Raven Press, 1979.
- Eskey, C. J., Wolmark, N., McDowell, C. L., Domach, M. M., and Jain, R. K. Residence time distributions of various tracers in tumors: implications for drug delivery and blood flow measurement. *J. Natl. Cancer Inst.*, 86: 293–299, 1994.
- Thompson, H. K., Stramer, C. F., Whalen, R. E., and MacIntosh, H. D. Indicator transit time considered as a γ variate. *Circ. Res.*, 14: 502–515, 1964.
- Nyquist, H. Certain topics in telegraph transmission theory. *Trans. Am. Inst. Elect. Engrs.*, 47: 617ff, 1928.
- Workman, P., and Graham, M. A. *Pharmacokinetics and Cancer Therapy*. Palinview, NY: Cold Spring Harbor Laboratory, 1993.